FATIGUE AND QUANTITATIVE FRACTOGRAPHY OF AN AL-6061 MATRIX COMPOSITE

B. R. CRAWFORD and J. R. GRIFFITHS*
School of Engineering and Technology, Deakin University, Geelong, Australia 3217
**Co-operative Research Centre for Alloy Solidification Technology (CAST)*
CSIRO Division of Manufacturing Technology, PO Box 883, Kenmore, Australia 4069

ABSTRACT

As part of a study on fatigue of Comral-85™†, a metal matrix composite, measurements have been made to relate crack growth rates and the area fraction of reinforcement, A_f, appearing on the fracture surface. Crack growth rates were similar to those observed for other metal matrix composites while A_f was found to be proportional to K_{max}^2. This confirms previous observations reported in the literature; however, the present data are of higher quality due to the use of fatigue crack growth specimens instead of the fatigue life specimens used in previous studies. The present methods also allowed an examination of the effect of stress state on reinforcement fracture. A_f was observed to decrease as the stress state changed from plane strain (at the centreline of the specimen) to near plane stress (near the edges).

KEYWORDS

Metal matrix composites, Comral-85™, fatigue crack growth, quantitative fractography

INTRODUCTION

Metal matrix composites have received a great deal of research attention during the last decade. This is mainly due to the large degree of control over their properties; in particular, the specific strength and stiffness. However, the limited ductility and low fracture toughness of composites has meant that a great deal of research has concentrated on the optimisation of the properties. In particular, the fatigue crack growth and fracture toughness of composites have been extensively investigated.

In the present paper some data are reported for fatigue crack growth in Comral-85™, a composite developed in Australia (Couper and Xia, 1991). The study examined the growth rates of fatigue cracks as a function of loading conditions, the effect of crack closure on crack growth and the interaction of the growing fatigue crack with the reinforcement particles.

---

† Comral-85™ and Micral-20™ are trademarks of Comalco Aluminium Pty Ltd of Australia

EXPERIMENTAL MATERIAL AND METHODS

Experimental Material

The material studied was Comral-85™, a metal matrix composite consisting of an AA-6061 matrix reinforced with 19% by volume of Micral-20™ microspheres. These are an unique reinforcement. They are, in contrast to particulate reinforcements of silicon carbide and alumina, spherical, polycrystalline and consist of several different phases. These phases are: mullite (77 vol%), alumina (19 vol%) and pseudo-brookite (4 vol%). The average diameter of the Micral-20™ particles was 25 μm. This places them in the upper reaches of the size range of reinforcements used in metal matrix composites.

The Comral-85™ was manufactured by adding the reinforcement to molten matrix alloy. After casting into a 300 mm diameter billet, it was extruded to a 75x25 mm rectangular cross-section bar. This was then heat-treated to peak aged condition. The heat-treatment consisted of solution treatment for 90 minutes at 530°C, followed by cold water quenching, pre-ageing at room temperature for 20 hours during which a tensile plastic pre-strain of 1.5% was applied and finally, ageing for 16 hours at 175°C. The purpose of the pre-straining was to reduce the residual stresses that resulted from quenching after solution treatment; the pre-strain did not crack any of the reinforcement particles nor did it affect the ductility of the aged material (Crawford, 1996b). The resultant mechanical properties are shown in Table 1.

Table 1: Mechanical properties of Comral-85™

Orientation	E (GPa)	$\sigma_{0.2}$ (MPa)	σ_{TS} (MPa)	ε_{TS} (%)	Hardness (HVN)
Longitudinal	85	309	340	4.1	135
Transverse	85	318	340	2.8	135

Experimental Methods

Fatigue test were conducted using compact tension specimens (ASTM E647-91) of 10 mm thickness and 60 mm width on an Instron 1342 servohydraulic testing machine. Crack lengths were measured using the compliance method and confirmed with visual measurements. Crack closure levels were estimated from load-displacement data collected during testing and analysed using the deviation from linearity method (Allison *et al.*, 1988). All fatigue tests were conducted under controlled ΔK and K_{max} conditions.

Fractographic examination was performed using a JEOL 6400F scanning electron microscope. The fracture surfaces were examined at points which were identified from the records of fatigue testing as having being produced under specific conditions. These points were then located using a point location method developed for the task (Crawford, 1996a). The area fraction, A_f, of reinforcement on the these fracture surfaces was quantified using the point count procedure described in ASTM E562. A total of 60 fields of 25 points were examined for the A_f versus K_{max} investigation while for the A_f versus stress state investigation (i.e., measuring the variation of A_f across the thickness of the sample) only 15 fields were examined. This gave 95% confidence intervals of ±2% and ±4% respectively.

RESULTS

Fatigue Crack Growth

The relationship between the fatigue crack growth rates and ΔK_{eff}, the effective stress intensity factor, is shown in Fig. 1. As can be seen, the data show the typical near-threshold and Paris Law regions. The extrinsic (or nominal) fatigue threshold (ΔK_{th}) at R = 0.1 is 3.6 MPa√m while

the intrinsic fatigue threshold ($\Delta K_{eff,th}$) is 1.7 MPa√m. The Paris Law exponent is 3.2. These values are in the middle of the range of values reported in the literature for AA-6061 based composites (Levin and Karlsson, 1991; Ishii *et al.*, 1991; Yu *et al.*, 1990). As in other metal matrix composites, the Paris Law region is limited to a small range of ΔK_{eff} due to the low fracture toughness of the composite. It should be noted that, just as for steels (Gray *et al.*, 1983), aluminium alloys (Clerivet and Bathias, 1988) and titanium alloys (Allison and Williams, 1985), the effect of load ratio on fatigue crack growth rates can be rationalised as the result of crack closure. This is demonstrated by the data in Fig. 1 which derive from tests conducted at R = 0.1 and R = 0.5 as well as constant ΔK tests conducted at 5 MPa√m with R values between 0.1 and 0.6.

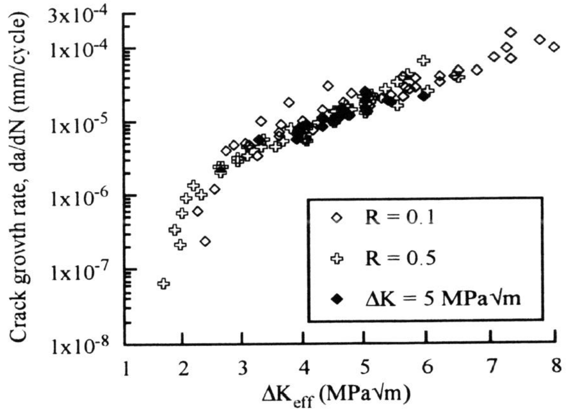

Fig. 1: Fatigue crack growth data for Comral-85™ as a function of ΔK_{eff} and test type.

Quantitative Fractography

Effect of loading condition. The quantitative fractography results for Comral-85™ are shown in Fig. 2. This figure plots A_f, the area fraction of reinforcement on the fracture surface, as a function of $(K_{max})^2$, where K_{max} is the maximum stress intensity factor applied during the fatigue cycle. The vast majority of particles observed on the fracture surface were fractured; decohesion of the matrix-reinforcement interface was seldom seen. The data in Fig. 2 derive from several different types of test, as indicated in the legend. These test types are (i) variable ΔK, R = 0.1 tests, (ii) variable ΔK, R = 0.5 tests and (iii) a constant K_{max} (= 8.9 MPa√m) test where ΔK was varied between 4.4 and 8 MPa√m. As can be seen, A_f is controlled by K_{max} and is independent of ΔK_{eff}. The line through the data in Fig. 2 is a linear least squares fit of the equation $A_f = \alpha K^2_{max} + \beta$ to the data. The values of α and β are 1.1×10^{-3} (MPa√m)$^{-2}$ and 1.1×10^{-1} respectively. The correlation coefficient of this fit, R^2, is 0.906 which is extremely good for experiments of this type. This is strong evidence that A_f is indeed related to K_{max}^2 and the size of the monotonic plastic zone as suggested by Bonnen *et al.* (1991) and Hall *et al.* (1994). These results show that the character of the fracture surface is not controlled by ΔK_{eff}, that is, by the rate of fatigue crack growth. Instead, it is controlled by a static fracture process, the fracture of the reinforcement.

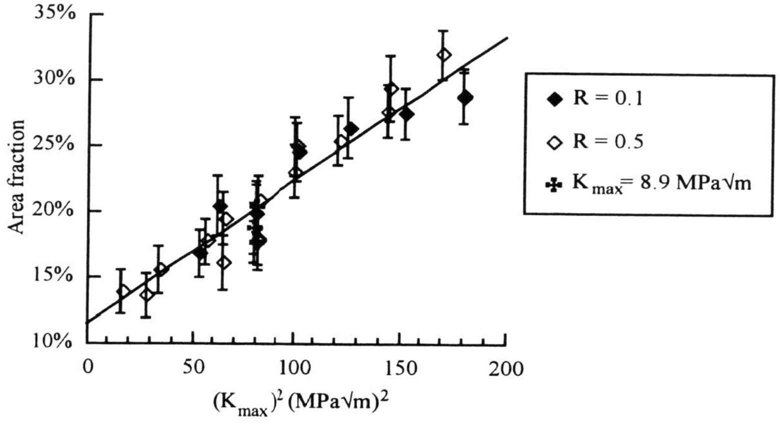

Fig. 2: Fit of equation $A_f = \alpha K^2_{max} + \beta$ to the area fraction results for Comral-85™. The solid line is the least squares fit of the equation to the data. The coefficient of correlation, R^2, is 0.906.

Effect of stress state. The effect of stress state on particle fracture was studied by quantifying A_f across the width of a specimen. Plane strain conditions prevailed at the centre of the specimens, while towards the edges of the specimen there would have been an approach to plane stress. The results of this investigation are shown in Fig. 3. As in Fig. 2 the error bars indicate 95% confidence intervals. In this case the 95% confidence interval is ±4% due to the reduced number of fields examined. As can be seen, A_f decreased as the stress state changed from plane strain, at the specimen's centreline, to near plane stress at the edges. The magnitude of this change was increased by an increase in K_{max}.

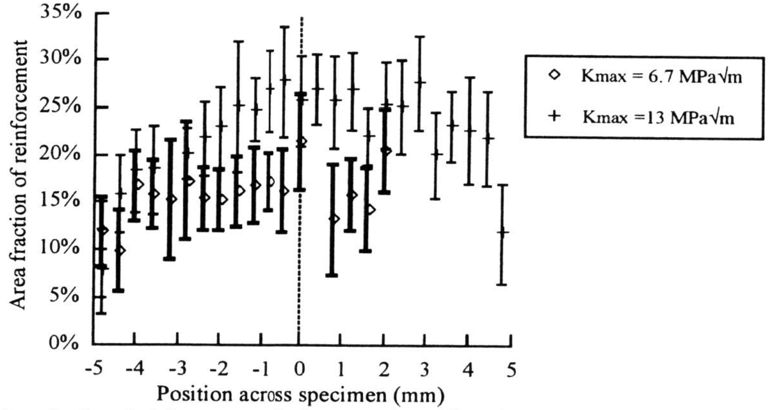

Fig. 3: Projected area fraction of reinforcement on the fracture surface of Comral-85™ as a function of distance from the centreline of the specimen (which is indicated by the zero on the x-axis). The specimen was approximately 10 mm thick. Error bars indicate 95% confidence intervals.

DISCUSSION

The data presented here, when considered separately, can be explained fairly readily. The relationship between A_f and K_{max}^2, Fig. 2, suggests that the probability of particle fracture and therefore A_f is related to the size of the monotonic crack-tip plastic zone, whose size is also proportional to K_{max}^2. This suggests that particle fracture is the result of shear strain. On the other hand, the A_f versus stress state results, Fig. 3, suggest that A_f increases with increasing hydrostatic stress. This is despite the large increase in the monotonic plastic zone size that accompanies the transition from plane strain to plane stress. These two arguments will now be developed separately.

To rationalise the effect of K_{max} on A_f it is proposed that it is not the absolute value of A_f that is significant so much as $\Delta A_f/A_o$, where $\Delta A_f = A_f - A_o$ and A_o is the value that would be found on a crack which did not deviate from its plane - i.e., the average value for the material, which in this case is 19%. If the particles had the same elastic and plastic properties as the matrix they would be invisible to the crack and $\Delta A_f/A_o$ would always be zero. However, this behaviour is not observed. Figure 2 shows that a crack growing with a small plastic zone deviates from its plane, presumably so as to avoid particles, $\Delta A_f/A_o < 0$; when the plastic zone is large the crack also deviates from its plane but this time seeks out particles, $\Delta A_f/A_o > 0$. This behaviour can be qualitatively understood as follows. When the plastic zone is small there is only a small probability that a particle is fractured by the stress and strain intensification ahead of the crack. In such cases the particles (which have a Young's modulus three times that of the matrix) act to deflect the crack since the value of K at the crack tip is reduced by the stiff particles. However, when the plastic zone is large the probability of particle fracture is high, with particles lying in the crack plane and to either side of it being broken; consequently the crack is attracted to these regions of, effectively, zero stiffness. This argument is, of course, only qualitative. At present there exists no quantitative prediction of either the slope, α, of the line in Fig. 2 nor of the intercept, β, at K_{max} equals zero. Comparison of the present results with data for metal matrix composites reinforced with silicon carbide particles (Bonnen *et al.*, 1991; Hall *et al.*, 1994) shows that Micral-20™ is more prone to fracture than SiC_p at a given value of K_{max}. It should be noted, however, that Hall *et al.* and Bonnen *et al.* studied composites with AA-2124 and AA-2175 matrices respectively. These matrix alloys are high strength aluminium alloys while the AA-6061 used in Comral-85™ is only a moderate strength alloy. This prevents direct comparison of the fracture of silicon carbide reinforcement with that of Micral-20™. The combination of a higher A_f for a given K_{max} in a weaker matrix alloy suggests, however, that Micral-20™ is more prone to fracture than silicon carbide.

It should be noted that the small range of K_{max} available to us ($4 \leq K_{max} \leq 13.5$ MPa√m) means that the goodness of fit of the quadratic equation may be deceptive. A linear relation between A_f and K_{max} is nearly as good. The quadratic form is preferred partly because fracture traditionally scales with K^2 but also because the data of Hall *et al.* and of Bonnen *et al.* clearly support the quadratic relation.

Examination of Fig. 3 shows that A_f decreased as the stress state changed from plane strain to near plane stress. This change is most pronounced in the K_{max} = 13 MPa√m results. A much smaller and, indeed statistically insignificant, change can be observed in the K_{max} = 6.7 MPa√m results. The difference between the two sets of data suggests that the change in A_f with position across the specimen is indeed the result of a change in stress state. Here it is suggested that the penetration of near-plane stress conditions into the specimen's thickness increases as K_{max} increases.

It is not surprising that particle fracture should be more prevalent under plane strain conditions since plane strain is associated with a high component of hydrostatic tension and this will encourage fracture although, at the same time, it is noted that the plastic zone size is smaller in plane strain. The data in Figs. 2 and 3, taken together, show that particle fracture is determined by both the plastic zone size and by the hydrostatic component of stress. Further work is in progress to separate the two effects.

CONCLUSIONS

The following conclusions can be drawn from this work on Comral-85™:

1. The area fraction of reinforcement on the fatigue fracture surface is determined by K_{max} and not by ΔK_{eff}. Here is a case where fracture surface morphology is not related to the rate of crack growth.
2. At low K_{max} the crack avoids the reinforcement and at high K_{max} it is attracted to it.
3. The area fraction of reinforcement on the fracture surface is higher in the plane strain region of the plastic zone than in the plane stress region.

ACKNOWLEDGMENTS

The authors are grateful to Comalco Research Centre, Thomastown, Australia, 3074 for the supply of experimental material and for financial support. In addition, we thank the Co-operative Research Centre for Alloy Solidification Technology (CAST) for financial support.

REFERENCES

Allison, J.E., Ku, R.C. and Pompetski, M.A. (1988). A comparison of measurement methods and numerical procedures for the experimental characterisation of fatigue crack closure. In: *Mechanics of Fatigue Crack Closure, ASTM Special Technical Publication 982*, (J.C. Newman and W. Elber, eds.), pp. 171-185, American Society for Testing and Materials, Philadelphia, PA, USA.

Allison, J.E. and Williams, J.C. (1985). The role of crack closure in rationalising the variations in fatigue crack growth behaviour in titanium alloys. In: *Titanium Science and Technology, 5th International Conference* (G. Luetjering, U. Zwicker and W. Bunk, eds.), Vol. 4, pp. 2243-2251. DGM Publishers, Obervsed, Federal Republic of Germany.

ASTM (1994a), E562-89: Standard test method for determining volume fraction by systematic manual point count. *Annual Book of ASTM Standards*, Vol. 03.01, pp. 502-706 American Society for Testing and Materials, Philadelphia, PA, USA.

ASTM (1994b), E647-93: Standard test method for measurement of fatigue crack growth rates. *Annual Book of ASTM Standards*, Vol 03.01, pp. 569-596 American Society for Testing and Materials, Philadelphia, PA, USA.

Bonnen, J.J., Allison, J.E. and Jones, J.W. (1991). Fatigue behaviour of a 2XXX series aluminum alloy reinforced with 15% v/o SiC_p, *Metallurgical Transactions A*, **23A**, 1007-1019.

Clerivet, A. and Bathias, C. (1988). Influence of some mechanical parameters on the crack closure effect in fatigue crack propagation in aluminium alloys. In: *Mechanics of Fatigue Crack Closure, ASTM Special Technical Publication 982* (J.C. Newman and W. Elber, eds.), pp. 583-597, American Society for Testing and Materials, Philadelphia, PA, USA.

Couper, M.J. and Xia, K. (1991). Development of a microsphere reinforced metal matrix composite. In: *Proceedings of 12th Risø International Symposium* (N. Hansen, D.J. Jensen, T. Leffers, H. Lilholt, T. Lorentzen, A.S. Pedersen and B. Ralph, eds.), pp. 291-298. Risø National Laboratory, Roskilde, Denmark.

Crawford, B.R. (1996a). A method for the location of specific points on surfaces in the SEM. *Journal of Microscopy*, **181**, 18-22.

Crawford, B.R. (1996b). Fatigue of an Al-6061 matrix composite. PhD Thesis, The University of Queensland, Australia.

Gray, G.T., Williams, J.C. and Thompson, A.W. (1983). Roughness-induced crack closure: an explanation for microstructurally sensitive fatigue crack growth. *Metallurgical Transactions A*, **14A**, 421-433.

Hall, J.N., Jones, J.W. and Sachdev, A.K. (1994). Particle size, volume fraction and matrix strength effects on fatigue behaviour and particle fracture in 2124 aluminum-SiC_p composites. *Materials Science and Engineering*, **A183**, 69-80.